Endocytic reawakening of motility in jammed epithelia

Chiara Malinverno, Salvatore Corallino, Fabio Giavazzi, Martin Bergert, Qingsen Li, Marco Leoni, Andrea Disanza, Emanuela Frittoli, Amanda Oldani, Emanuele Martini, Tobias Lendenmann, Gianluca Deflorian, Galina V. Beznoussenko, Dimos Poulikakos, ONG Kok Haur, Marina Uroz, Xavier Trepat, Dario Parazzoli, Paolo Maiuri, Weimiao Yu, Aldo Ferrari , Roberto Cerbino, Giorgio Scita

List of Contents

1. Supplementary Figure Legends

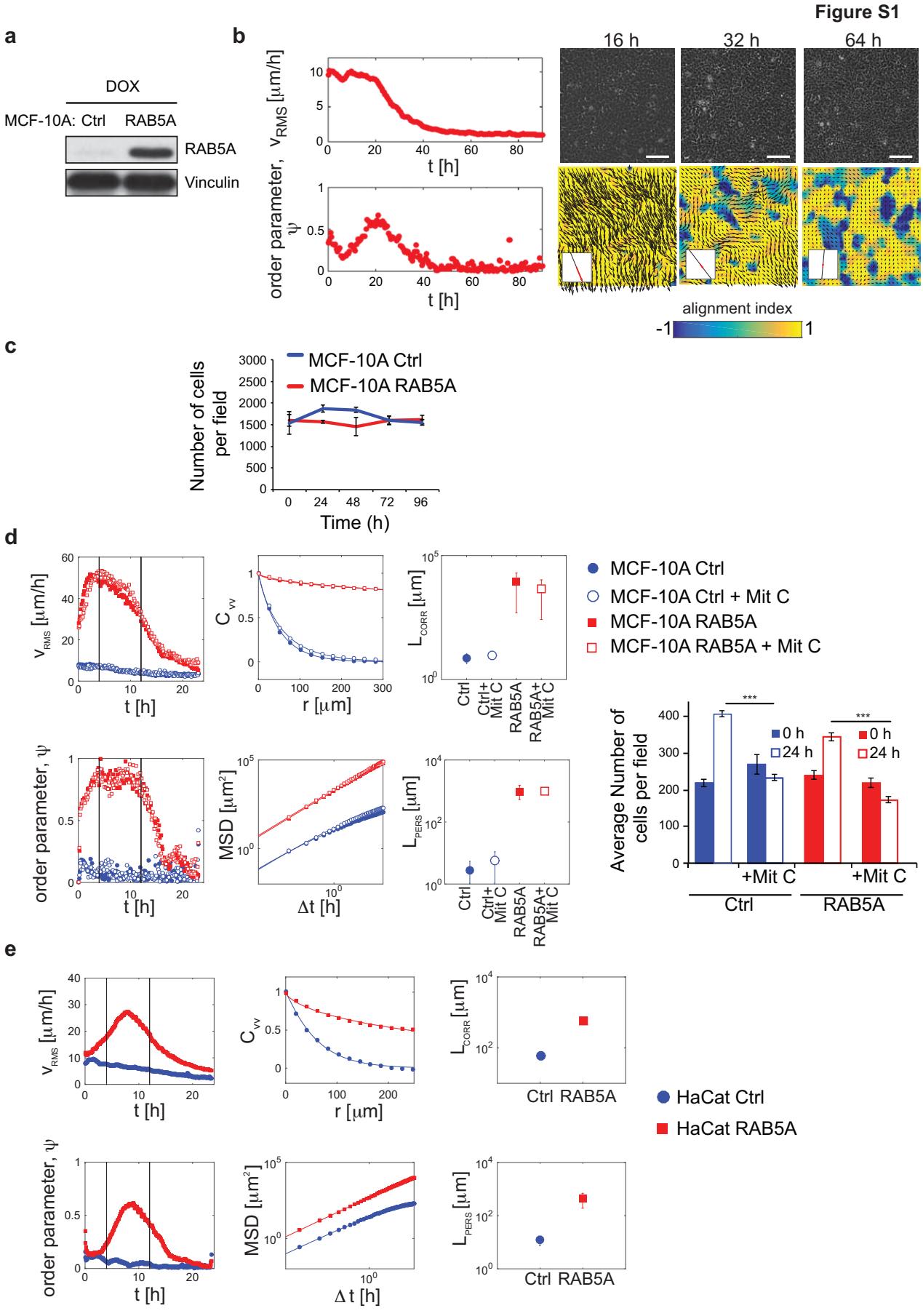

Supplementary Figure 1. RAB5A induces long-range collective motility in different epithelial

cells

(a) Immunoblotting of total lysates of doxycycline-treated control and RAB5A-MCF-10A using the indicated antibodies. Vinculin was used as loading control.

(b) Sub-confluent control MCF-10A cells were monitored by time-lapse phase contrast microscopy for 81 h (Supplementary Movie 1) and analysed by PIV to determine the local prevalent direction of motion resulting in velocity field's vectors. *Left*: temporal evolution of the root mean square velocity (*top graph*) and of the order parameter (*bottom graph*) of Ctrl monolayer. *Right*: three snapshots of the monolayer (*top panels*) and corresponding velocity fields (*bottom panels*), taken respectively 16, 32 and 64 h after the beginning of the experiment. Scale bar, 100 μm. The red arrow in the inset of each velocity field represents the corresponding mean vectorial velocity $\vec{v}_0$. The colours in the velocity maps reflect the alignment with respect to the mean velocity, quantified by the parameter $a(x) = (\vec{v}(x) \cdot \vec{v}_0)/(vv_0)$.

(c) Proliferation curves of doxycycline-treated control and RAB5A MCF-10A cells seeded at high (750,000/3.7 cm^2)-density and monitored by time-lapse phase contrast microscopy for 4 days. Every 24 h cells were counted and expressed as n of cells/field of view. Data are the mean ± SD (n=5/condition in three independent experiments).

(d) Doxycycline-induced control and RAB5A-MCF-10A cells seeded at jamming density and treated or not with mitomycin C were monitored by time-lapse phase contrast microscopy for 24 h (Supplementary Movie 4). Results of the PIV analysis performed on monolayers; from left to right and from top to bottom: temporal evolution of the mean square velocity v_{RMS}, velocity correlation functions $C_{VV}(r)$, corresponding correlation length L_{corr}, temporal evolution of the order parameter ψ, mean square displacements (MSD) and corresponding persistence length L_{pers}. The efficacy of mitomycin C was assessed by monitoring the number of cells seeded at sub-confluency and exponentially growing over a 24 h period. Data are the average number of cell/field of view and are the mean±SD (n=10 fields of view/condition in there independent experiments). ***$p < 0.001$.

(e) Doxycycline-induced control and RAB5A-HaCat keratinocytes seeded at jamming density were monitored by time-lapse phase contrast microscopy for 24 h (Supplementary Movie 5). Results of the PIV analysis performed on Ctrl and RAB5A-expressing monolayers of keratinocytes, HaCat. From left to right and from top to bottom: temporal evolution of the mean square velocity v_{RMS}, velocity correlation functions C_{VV}, corresponding correlation length L_{corr}, temporal evolution of the order parameter ψ, mean square displacements (MSD) and corresponding persistence length L_{pers}.

For all PIV measurements, at least 5 movies/experimental condition were analysed in 3-12 independent experiments. In (d-e), vertical lines indicate the time interval used for the analysis of motility parameters.

Figure S2

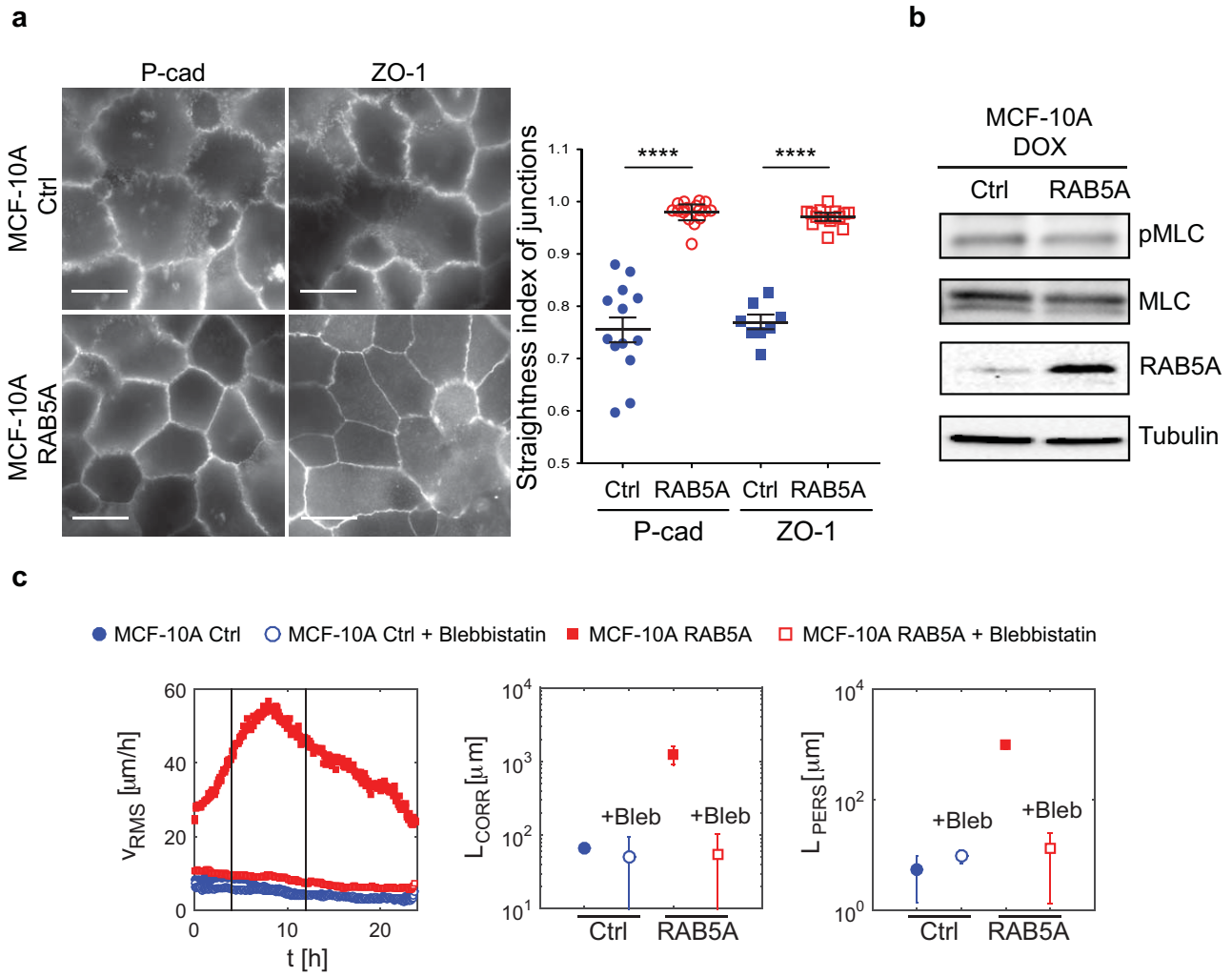

Supplementary Figure 2. Analysis of junctional proteins topology and expression

(a) *Left panels*: immunofluorescence localization of P-cadherin (P-cad) and ZO-1 in fully confluent and jammed control and RAB5A-MCF-10A monolayers after treatment for 16 h with doxycycline to induce transgene expression. Cells were fixed and stained for either P-cadherin (P-cad) or ZO-1. Scale bar, 20 µm. *Right graph*: the straightness index of junctions was quantified by the ratio of the distance between vertices of junctions to the total junctional length. Values ranged from 0 to 1, corresponding to wavy and linear junctions, respectively. Data are the mean ± SEM (n=12/condition of 4 independent experiments). **** $p < 0.0001$.

(b) Immunoblotting of total lysates of doxycycline-treated control and RAB5A-MCF-10A using antibodies against phosphorylated MLC (pMLC) and total MLC and RAB5A. Tubulin was used as loading control.

(c) *From left to right*: temporal evolution of the mean square velocity v_{RMS}, correlation length L_{corr} and persistence length L_{pers} were calculated by PIV analysis performed on doxycycline-induced control and RAB5A-MCF-10A cells seeded at jamming density and treated or not with Blebbistatin (25 µM) and monitored by time-lapse phase contrast microscopy. Data are the average

number of cells/field of view and are the mean ± SD (n=10 fields of view/condition in three independent experiments). ***$p < 0.001$.

Figure S3

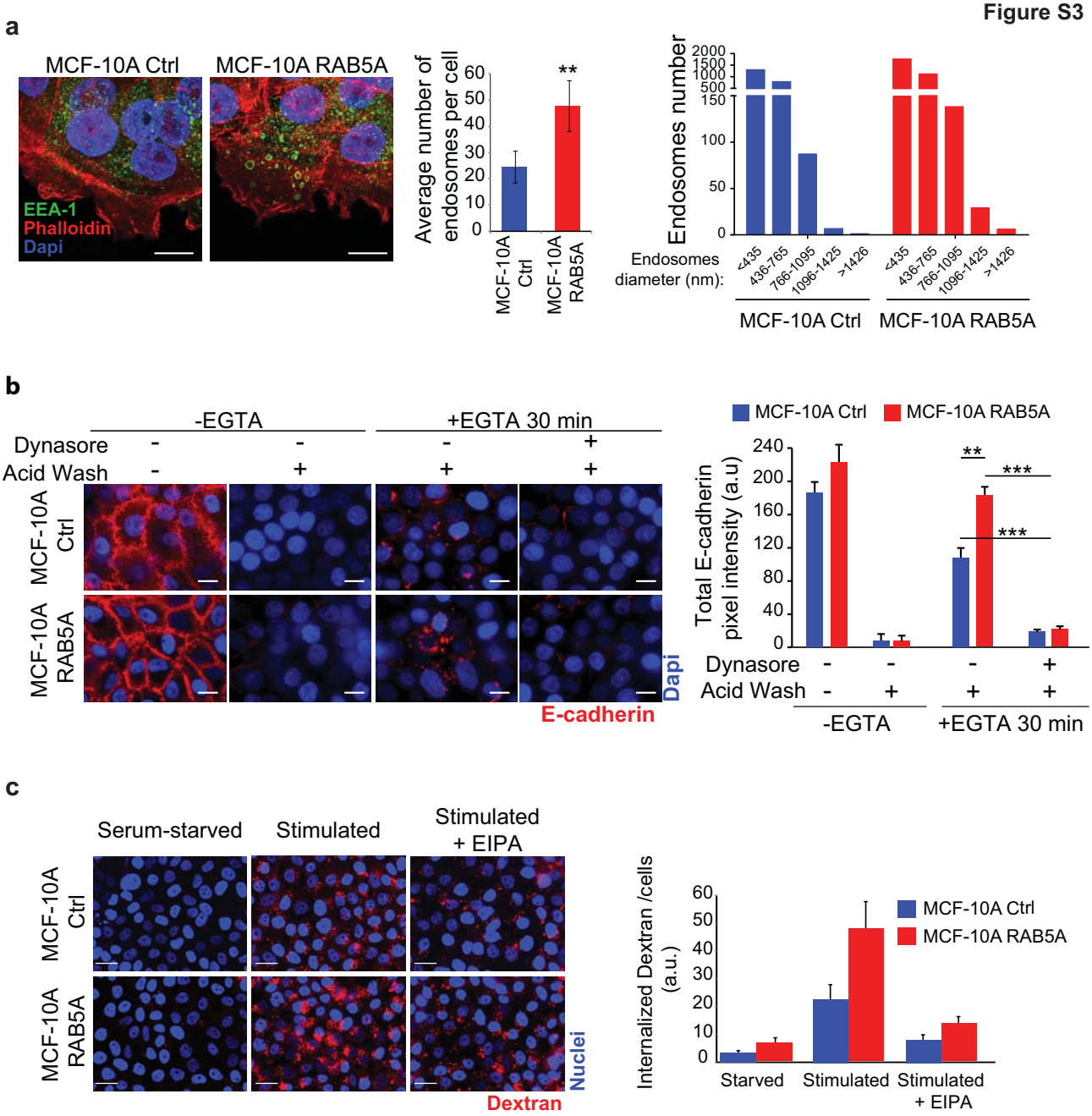

Supplementary Figure 3. RAB5A-induced endocytic perturbation

(a) *From left to right*: doxycycline-induced control and RAB5A-MCF-10A cells were fixed and stained to reveal nuclei with DAPI (blue), early endosomes with anti-EEA-1 antibody (green), and F-actin with TRITC-phalloidin (red). Scale bar, 5 µm. *Middle and right graphs*: CellProfiler software was used to quantify: the average number of EEA-1-positive endosomes/cell (*Left*) (n=200/cells out of more than 50 cells/condition analysed in three independent experiments, data are the mean ± SD); and the number of endosomes/each size category, indicated on the X-axis in nm. (*Right*) **p < 0.001.

(b) *Left panels*: E-cadherin internalization was measured in doxycycline-treated control and RAB5A-MCF-10A monolayers treated or not with the dynamin inhibitor Dynasore. Serum-starved

cells were pre-treated with Dynasore for 1 h, incubated at 4°C with the antibody recognizing the extracellular portion of human E-cadherin (HECD-1) and treated or not with EGTA for 30 minutes to induce E-cadherin internalization. Cells were acid-washed to remove surface-bound E-cadherin. Scale bar, 5 μm. *Right graph*: quantification of E-cadherin levels is reported as arbitrary units and is obtained by computing the total pixel intensity per number of cells. Data are the mean ± SD (n=30 fields/condition of three independent experiments). **$p < 0.001$, *** $p < 0.0005$.

(c) *Left panels*: to shown that rRAB5A promotes macropinocytosis, doxycycline-induced control and RAB5A-MCF-10A cells monolayers were starved for 16 h, pre-treated with EIPA [5-(N-Ethyl-N-isopropyl)amiloride] and incubated for 1 h with a mix of growth factors (EGF, HGF, EREG and AREG) (Stimulated) and tetramethylrhodamine-dextran. Cell were fixed and processed for epifluorescence to detect nuclei (blue) and TMR-dextran-positive macropinosomes (red), respectively. *Right graph*: quantification of macropinocytic uptake was performed by determining the intensity of TMR-dextran signal/cell and was expressed as arbitrary units. Data are the mean ± SD (n=150 cells/condition in three independent experiments).

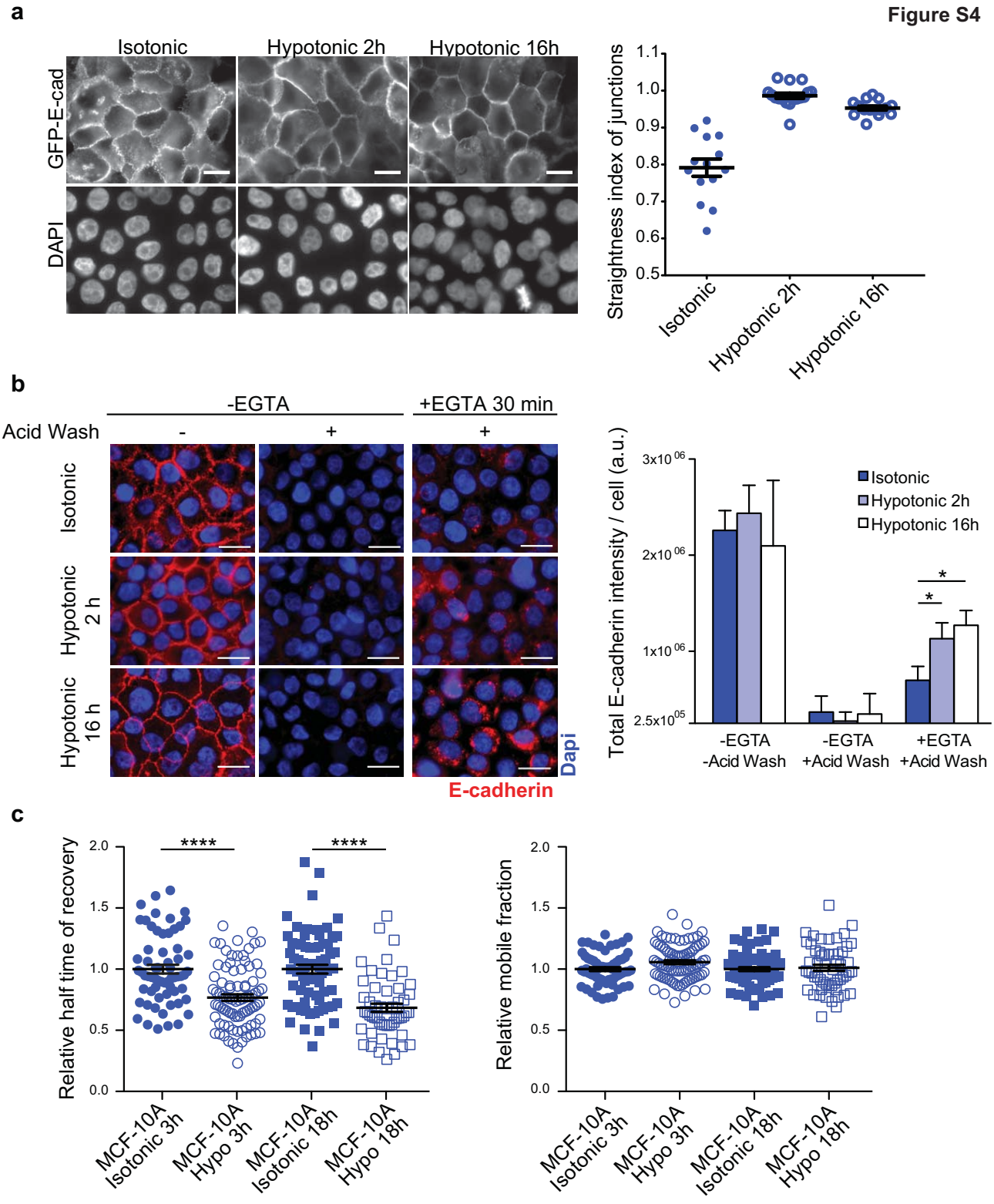

Supplementary Figure 4. Hypotonic treatment mimics RAB5A effects on junctional topology, endocytosis and E-cadherin dynamics

(a) *Left panels:* representative images of fully confluent and jammed control MCF-10A monolayers, stably expressing GFP-E-cadherin, treated with hypotonic media for the indicated time. Scale bar, 10 μm. *Right graph*: the straightness index of junctions was quantified as the ratio of the distance

between vertices of junctions to the total junctional length. Data are the mean ± SEM (n=70 cells in 3 independent experiments/condition). **** $p < 0.0001$.

(b) Left panels: E-cadherin internalization was measured in control MCF-10A monolayers treated or not with the hypotonic media. Monolayers were pre-treated with hypotonic media for the indicated time, incubated at 4°C with the antibody recognizing the extracellular portion of human E-cadherin (HECD-1) and treated or not with EGTA for 30 minutes to induce E-cadherin internalization. Cells were acid-washed to remove surface-bound E-cadherin. Scale bar, 5 μm. *Right graph:* quantification of E-cadherin levels is reported as arbitrary units and is obtained by computing the total pixel intensity per number of cells. Data are the mean ± SD (n=30 fields/condition of three independent experiments). *$p < 0.05$, paired Student's t-test.

(c) Hypotonic treatment increases E-cadherin dynamics. Dynamics of EGFP-E-cadherin measured by Fluorescence Recovery after Photobleaching (FRAP) in fully confluent control MCF-10A cells performed as described in Fig. 3a. The half time of recovery (left) and mobile fraction (right) calculated from the best fit curves (not shown) are expressed as mean ± SD (n=25 cells/condition of one representative experiment out of three with identical outcome). ****$p < 0.0001$, paired Student's t-test.

Figure S5

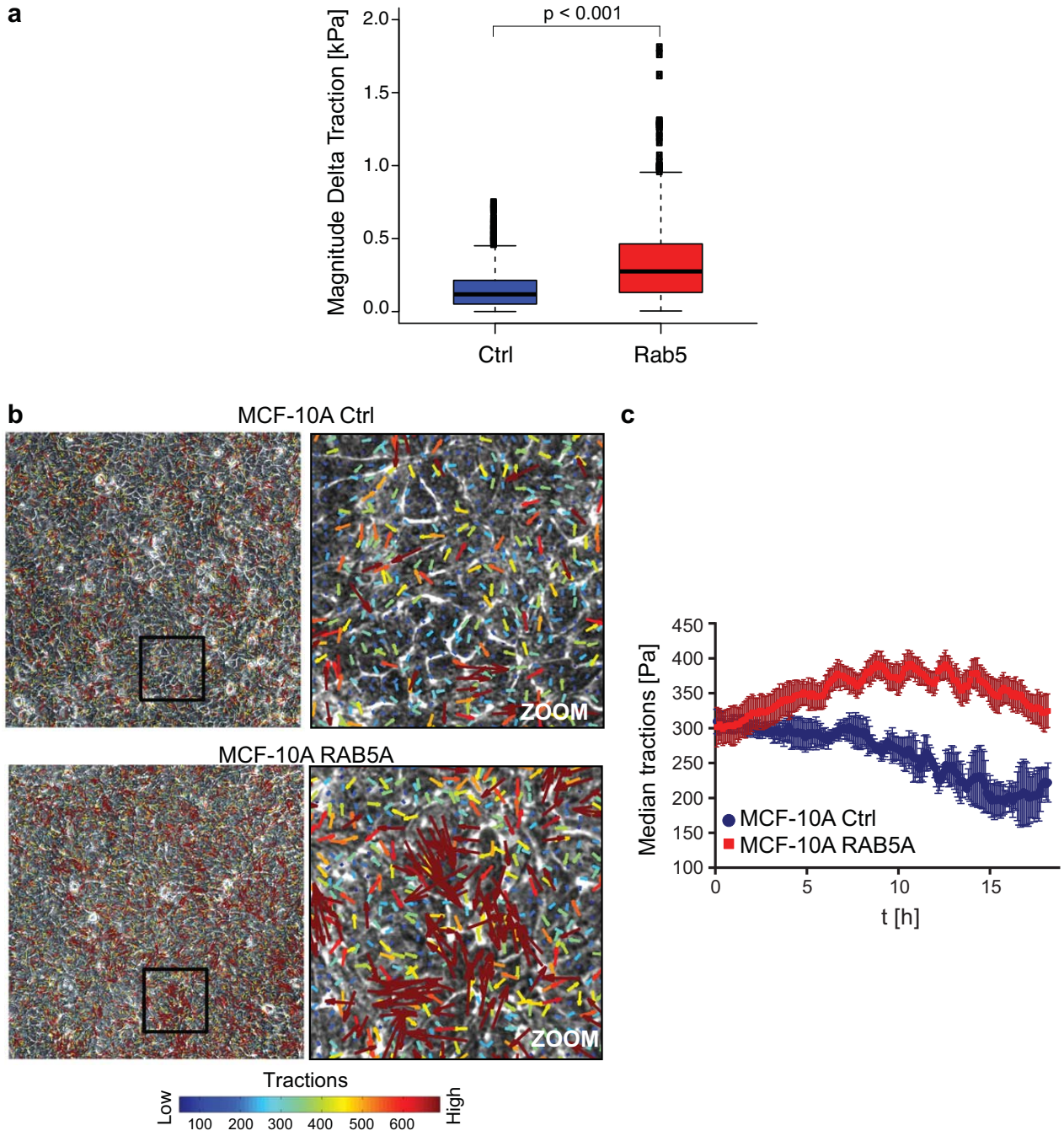

Supplementary Figure 5. RAB5A enhances monolayers traction forces

(a) Substrate tractions are more dynamic in RAB5A monolayers. Substrate tractions of control and RAB5A monolayers were measured using cTFM[1] as described in Fig. 4e (see Methods for details). The magnitude of the differences in tractions between consecutive timeframes was plotted for 9 random areas (5x5µm) and expressed in KPa out of 2 independent experiments. $p < 0.001$ was determined using Mann-Whitney-U-Test.

(b) Control (*top*) and RAB5A (*bottom*)-MCF-10A monolayers were seeded onto a collagen-coated polyacrylamide gel in which fluorescent beads were embedded[2]. Corresponding substrate traction forces were calculated by measuring fluorescent beads displacements. Colored arrows describe both

the direction and magnitude of the stresses exerted by cells on the substrate. The color code ranges from low (dark-blue) to high (dark-red) values of traction forces expressed in Pascal as indicated on the right graph. Higher magnification of the inset is shown on the right.

(c) Median value of control (blue) and RAB5A (red)-monolayer traction forces were calculated overtime. The graph shows the median mean value ± SD of 3 independent movies.

Figure S6

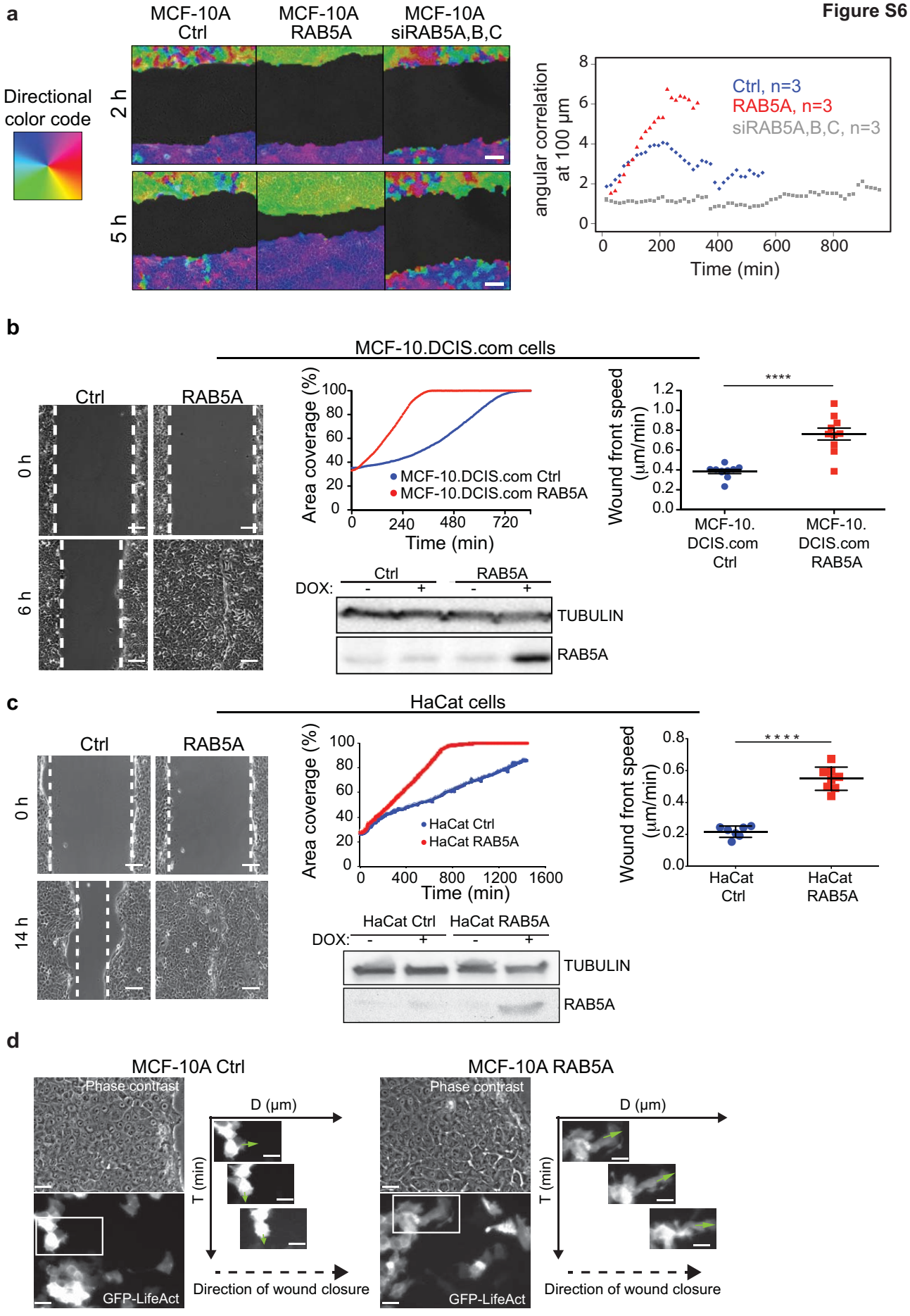
a
MCF-10A Ctrl
MCF-10A RAB5A
MCF-10A siRAB5A,B,C
Directional color code
2 h
5 h
angular correlation at 100 µm
Ctrl, n=3
RAB5A, n=3
siRAB5A,B,C, n=3
Time (min)
b
MCF-10.DCIS.com cells
Ctrl
RAB5A
0 h
6 h
Area coverage (%)
MCF-10.DCIS.com Ctrl
MCF-10.DCIS.com RAB5A
Time (min)
Wound front speed (µm/min)
****
MCF-10. DCIS.com Ctrl
MCF-10. DCIS.com RAB5A
DOX:
TUBULIN
RAB5A
c
HaCat cells
14 h
HaCat Ctrl
HaCat RAB5A
d
MCF-10A Ctrl
MCF-10A RAB5A
Phase contrast
GFP-LifeAct
D (µm)
T (min)
Direction of wound closure

Supplementary Figure 6. RAB5A promotes directed, collective motility of wounded monolayers

(a) RAB5A-induced acceleration of wound closure correlates with increased intercellular coordination. Cell Image Velocimetry (CIV) analysis of wounded, doxycycline-induced control, RAB5A-MCF-10A, and RAB5A, B and C silenced monolayers performed as in Fig. 1C (Supplementary Movie 20). Wound edges were detected in a segmentation step and cell layers were masked. Representative still images at t=2 and t=5 h are shown. The color code indicates direction of migration. Homogeneous colors indicate high coherence; in-homogeneous colors indicate in-coherent cell motility. Scale bar, 100 μm. *Right graph:* angular correlation plot was obtained by comparing the movement of cells with respect to their neighbours within a range of 100 μm. Data are the mean of 3 movies/condition from 3 independent experiments.

(b-c) Wound-healing assay of MCF-10.DCIS.com (b) and HaCat cells (c). Control and RAB5A expressing cells were grown to confluence and incubated in the presence of doxycycline for 16 h to induce transgene expression. Monolayers were scratched using a pipette tip and cell migration into the wound was monitored by time-lapse phase contrast microscopy for 24 h. Representative still images at the indicated times are shown on left panels. Dashed lines indicate the wound edge. Scale bar, 100 μm. Motility was quantified by measuring the percentage of area covered by cells overtime (MatLab software) (*middle top graph*) and the wound front mean velocity (*right top graph*). Data are the mean ± SD (n=5 movies/condition of 3 independent experiments). **** $p < 0.0001$.

Middle bottom panels: the expression of RAB5A was verified by immunoblotting using anti-RAB5A antibody. Tubulin was used as loading control.

(d) The extension and orientation of cryptic lamellipodia in wounded control and RAB5A-MCF-10A monolayers composed of GFP-LifeAct-expressing and non-expressing cells (1:10 ratio of EGFP-LifeAct expressing: non-expressing cells) was monitored by time-lapse fluorescence microscopy. Still phase contrast and fluorescent images from time-lapse sequences (Supplementary Movie 22) are shown on the left. Cryptic lamellipodia located behind the leading edge of the wound (indicated in the boxed insets) were monitored overtime by time-lapse fluorescence microscopy. Sequential still images of the boxed regions are shown on the right. Black dashed arrows indicate the direction of wound closure; green arrows indicate protrusions orientation. Scale bar, 40 μm.

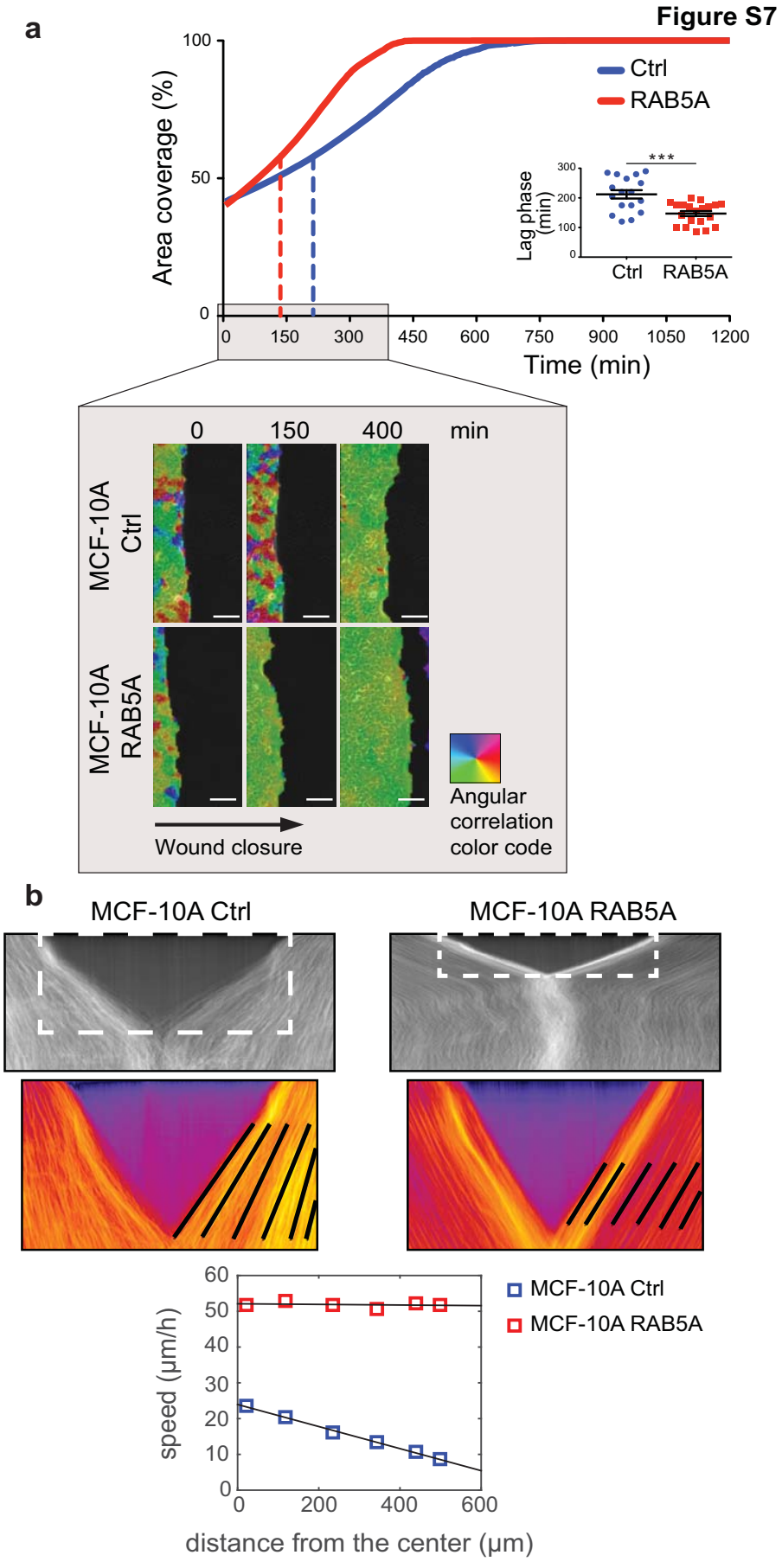

Supplementary Figure 7. Measurements of cell reorientation time

(a) Scratched wound migration of doxycycline-treated control and RAB5A-MCF-10A monolayers (see also representative Supplementary Movie 19). *Upper graph*: motility was quantified by measuring the percentage of areas covered overtime (MatLab software). The lag phase (*inset*) required to reach maximal velocity was computed after a double exponential fit of the velocity curves. Data are the mean ± SEM (n=5-to-10 fields of view out of 3 independent experiments). *** $p < 0.001$, Student's t-test. *Bottom images*, Representative Cell Image Velocimetry (CIV) analysis of wounded doxycycline-induced control and RAB5A-MCF-10A monolayers (see also representative Supplementary Movie 20). Wound edges were detected in a segmentation step and cell layers were masked. Representative still images at t=0, t=150 and t=400 min are shown. The colour code indicates direction of migration. Homogeneous colours indicate high coherence; in-homogeneous colours indicate in-coherent cell motility. Scale bar, 100 μm.

(b) *Top:* representative kymograph analysis of doxycycline-treated control and RAB5A-MCF-10A monolayers during scratch wound closure. Each line of the kymograph (*top images*) is obtained as the average (performed along the vertical direction, parallel to the wound edges) of images extracted from a sequence of 288 time-lapse images, taken at a frame rate of 30 frames per hour.

Dotted lines correspond to magnified regions shown in the bottom images. The height of the kymograph corresponds to the whole duration of the experiment (24 hours), while its width corresponds to the width of the original images (1.07 mm). *Centre:* rescaled portions of the kymographs before the wound closure. Black lines are guides for the eye superimposed to the stripes in the kymograph, corresponding to trajectories of specific features of the monolayer. *Bottom:* component of the velocity normal to the wound edge as a function of the distance from the centre of the wound for both Ctrl (blue symbols) and RAB5A (red symbols). Velocity is estimated from the slope of the stripes in the kymographs at different distances from the centre, immediately after the wound closure.

The data shown are obtained by averaging over 5 independent image sequences for each condition. The size of the symbols corresponds to the standard deviation associated to each data point.

2. Supplementary Movie Legends

Supplementary Movie 1. Fluid-like to glass-like transition of MCF-10A monolayer

Time-lapse phase contrast microscopy (*left*) and corresponding PIV analysis (*right*) of a confluent MCF-10A monolayer approaching a jamming transition phase. Pictures were taken every 10 min over an 82 h period. Scale bar, 100 μm. The red arrow in the inset represents the corresponding mean velocity $\vec{v}_0$, obtained as an average over the entire field of view. The color-map reflects the alignment with respect to the mean velocity, quantified by the parameter $a(x) = (\vec{v}(x) \cdot \vec{v}_0)/(v(x)v_0)$. $a = \pm 1$ when the local velocity is parallel (antiparallel) to the mean direction of migration.

Supplementary Movie 2. Collective streaming of control and RAB5A-MCF-10A cells in confluent monolayer

Collective locomotion of doxycycline-treated control and RAB5A-MCF-10A cells was monitored by time-lapse phase contrast microscopy (*top*) over a 22 h period, with pictures taken every 10 min. Corresponding PIV analysis is shown on the bottom. Scale bar, 100 μm. The red arrow in the inset represents the corresponding mean velocity $\vec{v}_0$, obtained as an average over the entire field of view. The color-map reflects the alignment with respect to the mean velocity, quantified by the parameter $a(x) = (\vec{v}(x) \cdot \vec{v}_0)/(v(x)v_0)$. $a = \pm 1$ when the local velocity is parallel (antiparallel) to the mean direction of migration.

Supplementary Movie 3. RAB5A re Supplementary awakens collective locomotion of jammed and kinetically arrested MCF-10A monolayer

Collective locomotion of control and RAB5A-MCF-10A monolayers plated at a jamming density was monitored by time-lapse microscopy. After 4 h, we added doxycycline, while keeping on recording monolayer motility by taking pictures every 10 min for the subsequent 38 hr. Scale bar, 100 μm.

Supplementary Movie 4. Cell proliferation does not account for collective migration of RAB5A-MCF-10A monolayers

Un-treated (*top*) and mitomycin C (1μg/ml)-treated (*bottom*), control and RAB5A-MCF-10A confluent monolayers were monitored by time-lapse phase-contrast microscopy. Frames were acquired every 10 min over a 24 h period. Scale bar, 100 μm.

Supplementary Movie 5. Collective streaming of control and RAB5A-HaCat cells in confluent monolayers

Collective locomotion of doxycycline-induced control and RAB5A-HaCat cells was monitored over a 24 h period, with pictures taken every 5 min. Scale bar, 100 μm.

Supplementary Movie 6. Single cell random migration of control- and RAB5A-MCF-10A cells

Random migration of control and RAB5A-MCF-10A individual cells was monitored in doxycycline-induced conditions over a 24 h period, with pictures taken every 5 min. Scale bar, 100 μm.

Supplementary Movie 7. Cell Image Velocimetry analysis of collective migration in control and RAB5A-MCF-10A monolayers

Collective locomotion of doxycycline-treated control and RAB5A-MCF-10A monolayers plated at jamming density was analyzed by Cell Image Velocimetry (CIV). Color code indicates direction of cell movement within the confluent monolayer. Homogeneous colors indicate high coherence; in-homogeneous colors indicate less coherent dynamics. Control and RAB5A-MCF-10A cells were compared over a 6 h period, with pictures taken every 5 min. Scale bar, 100 μm.

Supplementary Movie 8. RAB5A increases junctional tension in MCF-10A confluent monolayers

Nanoablation of cell-cell junctions in control and RAB5A-MCF-10A monolayers stably expressing EGFP-E-cadherin. Control MCF-10A monolayer in hypotonic condition has been used as positive control of the presence of local junctional tension. Pictures were taken every 3 sec. Scale bar, 10 μm.

Supplementary Movie 9. E-cadherin mobility in MCF-10A junctions is increased in RAB5A expressing monolayers

FRAP on control and RAB5A-MCF-10A monolayers stably expressing EGFP-E-cadherin. Representative photobleached regions are shown. Junctional recovery of control and RAB5A-MCF-10A cells was compared over a 244 sec period, with pictures taken every 4 sec. Scale bar, 5 μm.

Supplementary Movie 10. Collective motility in RAB5A-MCF-10A monolayer is suppressed by blocking dynamin-dependent endocytosis

Collective locomotion of control (*left panels*) and RAB5A-MCF-10A (*right panels*) cells was monitored in absence (*top*) or presence (*bottom*) of Dynasore 80 μM (+Dyn), over a 24 h period. Pictures were taken every 5 min. Scale bar, 100 μm.

Supplementary Movie 11. Inhibition of macropinocytosis affects RAB5A-mediated multicellular dynamics

Collective motility of control (*left panels*) or RAB5A-MCF-10A (*right panels*) cells was monitored by phase contrast time-lapse microscopy in absence (*top*) or presence (*bottom*) of macropinocytosis inhibitor EIPA 75 μM (+EIPA). Pictures were taken every 5 min, over a 24 h period. Scale bar, 100 μm.

Supplementary Movie 12. Fluid intake promotes collective motility of MCF-10A monolayers

Control MCF-10A confluent monolayer was treated with isotonic (*left panel*) or hypotonic (*right panel*) solutions and monitored by phase contrast time-lapse microscopy over a 24 h period. Pictures were taken every 5 min. Scale bar, 100 μm.

Supplementary Movie 13. Fluid intake modulation affects collective motility of RAB5A-MCF-10A monolayers

RAB5A-MCF-10A confluent monolayer was treated with isotonic (*left panel*), hypertonic (*middle panel*) or hypotonic (*right panel*) solutions and monitored by phase contrast time-lapse microscopy over a 24 h period. Pictures were taken every 10 min. Scale bar, 100 μm.

Supplementary Movie 14. RAB5A promotes the persistent extension of cryptic lamellipodia oriented along the motility direction in confluent monolayers

GFP-LifeAct and unlabeled MCF-10A cells were mixed to monitor the formation of cryptic lamellipodia in control and RAB5A-MCF-10A confluent monolayers. Pictures were acquired by phase contrast and fluorescence time-lapse microscopy every 90 sec over 2 h period. Scale bar, 50 μm.

Supplementary Movie 15. Inhibition of RAC1 activation affects the formation of polarized and persistent cryptic lamellipodia

GFP-LifeAct and unlabeled MCF-10A cells were mixed to monitor the formation of cryptic lamellipodia in control (*top panels*) and RAB5A-MCF-10A (*bottom panels*) confluent monolayers,

in absence or presence of RAC1 inhibitor 100 μM (+NSC23766). Pictures were taken every 30 sec, over a 3 h period. Scale bar, 15 μm.

Supplementary Movie 16. Inhibition of RAC1 activation impairs the motility of RAB5A-MCF-10A confluent monolayers

Collective locomotion of control (*left panels*) and RAB5A-MCF-10A (*right panels*) confluent monolayers was monitored in absence (*top*) or presence (*bottom*) of RAC1 inhibitor 100 μM (+NSC23766), over a 23 h period. Pictures were taken every 10 min. Scale bar, 100 μm.

Supplementary Movie 17. RAB5A increases strain fluctuations exerted by MCF-10A monolayers onto the substrate

Control (*top*) and RAB5A (*bottom*)-MCF-10A monolayers were seeded on cTFM substrates (elastic silicone substrates with fluorescent Quantum Dot nanodisc arrays)[1]. *Left*: cell motility and Quantum Dot nanodisc dynamics were monitored for about 3 h, taking pictures every 5 min. Fluorescent dots are shown in red and nuclei in green. *Right*: corresponding substrate traction magnitude maps were generated from Quantum Dot nanodisc displacements using a nonlinear FEM-based analysis[1]. The color code ranges from 0 to 15 kPa (dark-blue to dark-red). Scale bar, 15 μm.

Supplementary Movie 18. Changes in effective line tension and polarity reorientation efficiency determine different regimes in the monolayer dynamics

Left: example of a "liquid" state, not far from to the jamming transition, as obtained from the numerical simulations. Model parameters are the following: v_0=0.25, D_r=0.25, p_0=3.135, τ=8. *Right*: example of a "flowing liquid" state. Characterized by a lower effective line tension (p_0=3.8) and more efficient reorientation dynamics (τ=0.25), it exhibits the compresence of collective sheet migration and local topological rearrangements. The values of v_0 and D_r are the same of the previous example.

Supplementary Movie 19. RAB5A modulation affects directional collective migration of MCF-10A cells

Control (*left*), RAB5A-MCF-10A (*middle*), and RAB5A, B and C silenced (*right*) monolayers were scratched to induce directed cell migration during wound healing. Cells were monitored by phase contrast time-lapse microscopy over a 24 h period. Pictures were taken every 5 min. Scale bar, 100 μm.

Supplementary Movie 20. RAB5A-induced acceleration of wound closure correlates with increased cell-cell coordination

Phase contrast time-lapse movies of wounded, doxycycline-induced control, RAB5A-MCF-10A, and RAB5A, B and C silenced monolayers were analyzed by Cell Image Velocimetry (CIV). Pictures were taken every 5 min over about 17 hours period. Scale bar, 100 μm.

Supplementary Movie 21. RAB5A increases the extension of polarized and persistent protrusions

Control (*top*) and RAB5A-MCF-10A (*bottom*) confluent monolayers were scratched to monitor wound edge dynamics by phase contrast time-lapse microscopy. Pictures were acquired every 30 sec over 1 h period. Scale bar, 20 μm.

Supplementary Movie 22. RAB5A promotes the formation of oriented cryptic lamellipodia in cells at the leading front and 10 rows behind the wound edge

GFP-LifeAct and unlabeled control (top movies) or MCF-10A-RAB5A (bottom movies) cells were mixed to visualize the formation of cryptic lamellipodia in wound healing conditions. Left and right movies are epifluorescence and phase contrast image sequences, respectively. Images were acquired every 90 sec over 2 h period. Scale bar, 50 μm.

Supplementary Movie 23. RAB5A-MCF-10A monolayer flows like streams under physical constrains

Collective locomotion through 25 μm narrow PDMS channels of control (*top panel*) and RAB5A-MCF-10A (*bottom panel*) confluent monolayers was monitored by phase contrast time-lapse microscopy. Pictures were taken every 5 min, over a 24 h period. Scale bar, 100 μm.

Supplementary Movie 24. Zebrafish gastrulation

Live epiboly movements of control or RAB5A injected zebrafish embryos were monitored by phase contrast time-lapse microscopy. Pictures were taken every 5 min, over a 3 h period. Scale bar, 500 μm.

3. Definition of the numerical model

Cells in a confluent monolayer are modelled as self-propelled Voronoi objects, as described in[3]. Explicitly, the monolayer configuration is described by assigning the positions $\{\mathbf{r}_k\}$ of the N cell centres, acting as generators of a Voronoi tessellation of the plane. Each cell is identified with a Voronoi polygon. The k-th cell is subjected to a force $\boldsymbol{F}_k = -\nabla_k \mathrm{E}$, where ∇_k is the derivative with respect to the position of cell centre $\mathbf{r}_k$ and the energy E is given by

$$E = \sum_k [K_A(A_k - A_0)^2 + K_P(P_k - P_0)^2]$$

Here A_k and P_k are, respectively, the area and the perimeter of the k-th cell, A_0 and P_0 are, respectively, a target area and a target perimeter, and K_A and K_P are the area and perimeter moduli, respectively. This is the form assumed for the interaction energy both in the vertex model described in [3, 4]and in the self-propelled Voronoi model proposed by [3]. The interested reader is referred to these papers for a detailed discussion on the interpretation of the parameters. The cellular motion is determined by a combination of the external force $\boldsymbol{F}_k$ and a self-propelled term according to the equation:

$$\frac{d\boldsymbol{r}_k}{dt} = \mu \boldsymbol{F}_k + v_0 \boldsymbol{n}_k$$

where $\boldsymbol{n}_k$ is a unit vector giving the polarity direction of the cell, while μ and v_0 are constant. The angle θ_k describing the orientation of the polarity vector $\boldsymbol{n}_k$ obeys the following equation:

$$\frac{d\theta_k}{dt} = \eta_k - \frac{1}{\tau} f\left(\frac{d\boldsymbol{r}_k}{dt}, \boldsymbol{n}_k\right)$$

where $\eta_k(t)$ is a white noise with zero mean and variance $2D_r$ and $f(\boldsymbol{a}, \boldsymbol{b})$ is the angle between the vectors $\boldsymbol{a}$ and $\boldsymbol{b}$. This last equation incorporates a Vicsek-like alignment mechanism such that the cell polarity, tends to relax along the direction of the actual cell velocity with a characteristic time τ [5]. We note that in the limit $\tau \to \infty$ the here-described model coincides with the self-propelled Voronoi model proposed by[3]. The model can be made dimensionless by adopting $\sqrt{A_0}$ and $(\mu K_A A_0)^{-1}$ as the length and time unit, respectively. The remaining independent parameters are: the self-propulsion speed v_0 (which we set to 1), the rotational diffusion coefficient D_r (which we set to 0.25), the ratio $K_P/(A_0 K_A)$ (which we set to 1), the target shape index p_0 and the response time τ.

We performed numerical simulations with N=128 and N=256 cells, adopting periodic boundary conditions. Simulations are performed by direct integration of the equation of motion using the Euler's method. The integration step was set to $\Delta t = 0.1$. A typical simulation encompasses 10^4

integration steps. For each combination of the model parameters (p_0, τ) the dynamical state of the system has been assessed by estimating the long-time effective diffusion coefficient $D_{eff} = \lim_{\Delta t \to \infty} \langle |\boldsymbol{r}_k(t + \Delta t) - \boldsymbol{r}_k(t)|^2 \rangle / (4\Delta t)$, the average shape factor $q = \langle P_k / \sqrt{A_k} \rangle$ and the orientational order parameter ψ.

Supplementary Figure 8

Qualitative phase diagram obtained from simulations. Different dynamical states of the monolayer as a function of two control parameters: the target shape index p_0 (horizontal axis), which encodes the effective line tension at cell-cell junctions, and the inverse reorientation time τ^{-1}, which expresses the efficiency of the local alignment mechanism of the self-propelled velocities of the cells. Simulations show the presence of two transition lines. A first boundary (continuous blue line) separates the solid-like, jammed states (circles), for which mutual rearrangement of the cells are prevented and $D_{eff} \cong 0$, from "liquid" states, for which a non-zero long-time diffusivity is observed (squares). In agreement with [3], we found that the liquid-solid transition occurs when the shape factor q attains the critical value of $\cong 3.81$. A second (black) line marks the transition between "flowing states" (crosses), where directed collective migration is observed and the order parameter ψ is non-zero, and "non-flowing states" (dots), for which no long-range orientational order is present $\psi < 0.05$.

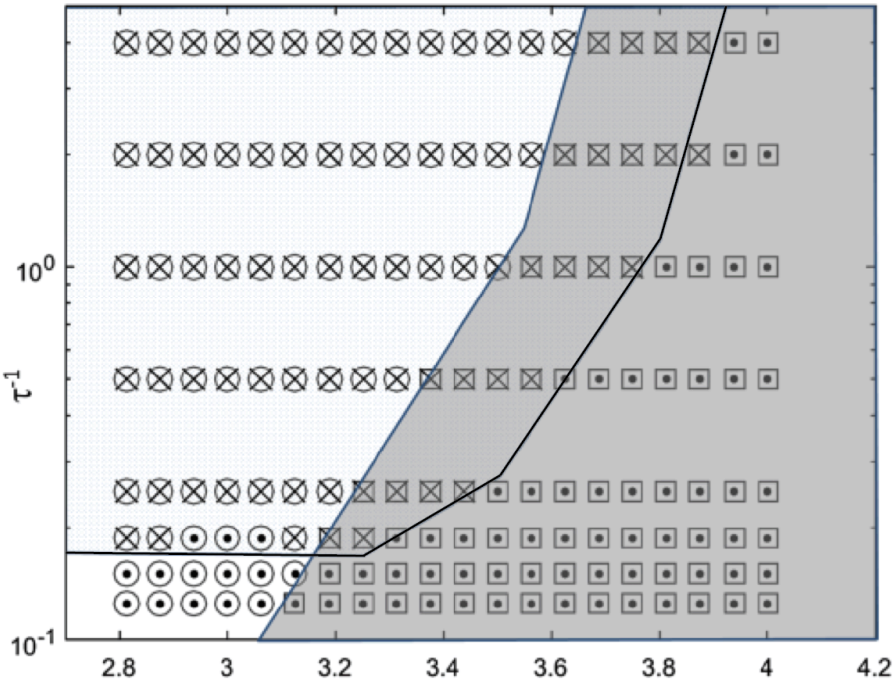

A more comprehensive discussion of the results of the simulations of the described model will be presented elsewhere.

3. Supplementary Methods

Plasmids, antibodies and reagents

Doxycycline-inducible pSLIK-neomycin (neo) and pSLIK-hygromycin (hygro) lentiviral vectors carrying RAB5A sequence were obtained by Gataway Technology (Invitrogen), following the manufacturer's protocol. The plasmid pBABE-puromycin (puro)-EGFP-H2B was provided by IFOM-Imaging Facility. pLL5.0 E-cadherin shRNA/mEcad–GFP vector was a gift from Alpha S.Yap (Division of Molecular Cell Biology, Institute for Molecular Bioscience, The University of Queensland, Australia). Lentiviral expression constructs pRRL-Lifeact-EGFP-puromicin (puro) was a gift of Olivier Pertz (University of Basel, Basel, Switzerland).

Mouse monoclonal antibodies raised against α−tubulin (#T5168) or vinculin (#V9131) were from Sigma-Aldrich; rabbit polyclonal anti-RAB5A (S-19, #sc-309), rabbit polyclonal anti-MLC2 (FL172, #sc-15370) and goat polyclonal anti-EEA-1 (N-19, #sc-6415) antibodies from Santa Cruz Biotechnology. Mouse monoclonal anti-HA1 was homemade. Rabbit polyclonal anti-ZO1 (#61-7300) antibody was from Invitrogen, mouse monoclonal anti-E-cadherin (#610181) and mouse monoclonal anti-P-cadherin (#610227) antibodies were from Transduction Lab. Rabbit polyclonal anti-phospho-MLC2 (Ser19, #3671) antibody was from Cell Signaling. Secondary antibodies conjugated to horseradish peroxidase were from Bio-Rad (#7074, #7076); Cy3-secondary antibodies from Jackson ImmunoResearch (#711-165-152, #715-165-150); DAPI (#D-1306) and AlexaFluor 488 (A-11055, A-21202) were from Thermo Fisher Scientific. TRITC- (#P1951) and FITC-(#P5282) conjugated phalloidin were from Sigma Aldrich.

NSC23766 (#S8031) was purchased from Selleckchem; Doxycycline Hyclate (#D9891), Dynasore Hydrate (#D7693), 5-(N-Ethyl-N-isopropyl) amiloride (EIPA, #A3085), Blebbistatin (#B0560) and Mitomycin C (#M0503) from Sigma Aldrich. For internalization assay, mouse-monoclonal E-cadherin / CDH1 antibody was purchased from Thermo Fisher Scientific (HECD-1, #13-1700). For macropinocytosis assay, Dextran, Tetramethylrhodamine, 70,000 MW was purchased from Thermo Fisher Scientific (#D1818).

Grids, osmium tetraoxide, paraformaldehyde and glutaraldehyde were purchased from Electron Microscopy Sciences (EMS, USA). Sodium cacodylate and Epoxy resin kit were purchased from Fluka (SIGMA, USA). Potassium ferrocyanide, ethanol and acetone were purchased from Carlo Erba (Italy), and Mat Tek dishes (P35G-1.5-14-C-GRID) from MatTek Corporation (USA).

Generation of lentiviral and retroviral particles

Packaging of lentiviruses or retroviruses was performed following standard protocols. Four batches

of viral supernatant were collected and filtered through 0.45 μm filters. Cells were subjected to four cycles of infection and selected using the appropriate antibiotic: neomycin for pSLIK-neo vector (150 μg/ml), hygromycin for pSLIK-hygro vector (100 μg/ml) or puromycin for EGFP-LifeAct or pBABE vectors (2 μg/ml). After several passages, stable bulk populations were selected and induced by Doxycycline Hyclate (2.5 μg/ml) in order to test: i) induction efficiency by Western Blotting and quantitative RT-PCR (qRT-PCR), and ii) the homogeneity of the cell pool by immunofluorescence staining.

RNA interference

Control-MCF-10A cells were seeded the day before to be 60-80% confluent at the time of transfection. siRNAs (small interfering RNAs) delivery was achieved by mixing 1 nM of specific siRNAs with Optimem and Lipofectamine RNAiMAX Transfection Reagent (Life Technologies). The following siRNAs were used for knocking down specific genes. All sequences are 5' to 3'. RAB5A, CAAGCCTAGTGCTTCGTTT; RAB5B, CGACATTACTAATCAGGAA and RAB5C, GGACAGGAGCGGTATCACA.

All siRNAs were purchased from Life Technologies. For each RNA interference experiment, negative control was performed with the same amount of scrambled siRNAs. Silencing efficiency was controlled by qRT-PCR.

Quantitative RT-PCR analysis

Total RNA was extracted using RNeasy Mini kit (Qiagen) and quantified by NanoDrop to assess both concentration and quality of the samples. Reverse transcription was performed using SuperScript VILO cDNA Synthesis kit from Invitrogen.

Gene expression was analysed using TaqMan Gene expression Assay (Applied Biosystems). 0.1 ng of cDNA was amplified, in triplicate, in a reaction volume of 25 μl with 10 pMol of each gene-specific primer and the SYBR-green PCR MasterMix (Applied Biosystems). Real-time PCR was performed on the 14 ABI/Prism 7700 Sequence Detector System (PerkinElmer/Applied Biosystems), using a pre-PCR step of 10 min at 95°C, followed by 40 cycles of 15 s at 95°C and 60 s at 60°C. Specificity of the amplified products was confirmed by melting curve analysis (Dissociation Curve TM; PerkinElmer/Applied Biosystems) and by 6% PAGE. Preparations with RNA template without reverse transcription were used as negative controls. Samples were amplified with primers for each gene (for details see the Q-PCR primer list below) and GAPDH as a housekeeping gene. The Ct values were normalized to the GAPDH curve. PCR experiments were performed in triplicate and standard deviations calculated and displayed as error bars. Primer assay

IDs were: GAPDH, Hs99999905_m1; RAB5A, Hs00702360_s1; RAB5B, Hs00161184_m1 and RAB5C, Hs00428044_m1.

Immunoblotting

For protein extraction, cells were lysed in JS buffer containing proteases and phosphatases inhibitors. Cell lysates were cleared by centrifugation at 13,000 rpm for 30 min at 4°C. Protein concentration was quantified by Bradford colorimetric protein assay. The same amount of protein lysates was loaded onto polyacrylamide gel in 5X SDS sample buffer. Proteins were transferred onto Protran Nitrocellulose Transfer membrane (Whatman), probed with the appropriate antibodies and visualized with ECL Plus western blotting detection reagents (GE Healthcare). Chemiluminescence was detected by ChemiDoc™ XRS+ System (Bio-Rad). Membrane blocking and incubation in primary or secondary antibodies were performed for 1h in TBS/0.1% Tween/5% BSA for antibodies recognizing phosphorylated proteins or in TBS/0.1% Tween/5% milk for antibodies recognizing the total proteins. Primary antibodies were diluted 1:1,000 and secondary antibodies 1:10,000 as suggested by the manufacturer.

Immunofluorescence

Cells were fixed in 4% paraformaldehyde (PFA) and permeabilized with 0.1% Triton X-100 and 1% BSA 10 minutes (except for EEA-1 staining, permeabilized with 0.02% Saponin and 1% BSA 10 minutes). After 1X PBS wash, primary antibodies were added for 1 hour at room temperature. Coverslips were washed in 1X PBS before secondary antibody incubation 1 hour at room temperature, protected from light. FITC- or TRITC-phalloidin was added in the secondary antibody step, where applicable. After removal of not specifically bound antibodies by 1X PBS washing, nuclei were stained with 0.5 ng/ml DAPI. Samples were post-fixed and mounted on glass slides in anti-fade mounting medium (Mowiol). Antibodies were diluted in 1X PBS and 1% BSA. Images were acquired by wide-field fluorescence microscope or confocal microscope, as indicated in figure legends.

E-cadherin staining was analyzed by confocal microscopy and images were processed to obtain the straightness index of the junction. “Junction length” was measured by tracking a straight line and “junction tracking” was obtained by tracking manually the same junction following its profile. The straightness index of the junction has been quantified as the ratio of the junction length and the junction tracking.

Electron Microscopy

For electron microscopy the cells were processed as previously described[6]. Briefly, the cells grown on Mat Tek dishes were fixed with a mixture of 4% paraformaldehyde and 2,5% glutaraldehyde in 0.2 M sodium cacodylate pH 7.2 for 2 h at RT. Afterwards, the cells were washed 6 times in 0.2 sodium cacodylate pH 7.2 at RT. Osmification followed: the cells were incubated for 1 h at RT with a 1:1 mixture of 2% osmium tetraoxide in distilled water and 3% potassium ferrocyanide in 0.2 M sodium cacodylate (pH 6.9) and then rinsed 6 times with the cacodylate buffer, for 5 min treated with 0.3% Thiocarbohydrazide in 0.2 M cacodylate buffer (pH 6.9) for 10 min, washed 3 times with 0.2 M cacodylate buffer (pH 6,9), treated with 1% OsO4 in 0.2 M cacodylate buffer (pH 6,9) for 30 min. Then, samples were rinsed with 0.1 M sodium cacodylate (pH 6.9) buffer until all traces of the yellow osmium fixative have been removed. The samples were then dehydrated: 3x10 min in 50% ethanol; 3x 10 min in 70% ethanol; 3x 10 min in 90% ethanol; 3x 10 min in 100% ethanol. The samples were subsequently incubated for 2 h in 1:1 mixture of 100% ethanol and Epoxy resin (Epon) at RT, the mixture was then removed with a pipette and finally samples were embedded for 4 h in Epoxy resin at RT. The resin was polymerized for at least 72 h at 60 °C in an oven. The samples embedded into resin were carefully picked up from glass and sectioned with diamond knife (Diatome, Switzerland) using Leica UC7 ultramicrotome. Sections (50-60 nm) were analysed with a Tecnai 20 High Voltage EM (FEI, The Netherlands) operating at 200 kV.

E-cadherin internalization with HECD-1 anti-E-cadherin Antibody

For HECD-1 anti-E-cadherin internalization, cells were grown on glass coverslips and starved in DMEM/F12 for 1 h before experiment. Samples were then incubated for 1 h at 4°C with anti-E-cadherin (HECD-1) IgG diluted in PBS solution. Where appropriate, cells were pre-treated for 1 h with 80 μM Dynasore before incubation with the HECD- 1 antibody. Coverslips were washed with ice-cold PBS to remove the unbound antibody and the media was replaced with pre-warmed culture medium containing 100 ng/ml EGF and 5% horse serum, in the presence or absence of EGTA 4 mM. After incubation at 37°C for 30 min, cells were washed with PBS and returned to 4°C. The residual surface-bound antibody was removed by acid washing (0.5 M acetic acid, 0.5 M NaCl). Cells were washed with PBS before fixation with 4% paraformaldehyde for 10 minutes at room temperature. Indirect immunofluorescence staining was performed on permeabilized cells by incubation with CY3-conjugated anti-mouse antibody and DAPI. Internalization of E-cadherin was quantified using ImageJ software.

Dextran Internalization Assay

Cells were plated on glass coverslips, without gelatin coating, and cultured in complete medium until a uniform monolayer had formed. Cells were concomitantly doxycycline-induced and starved in DMEM/F12+cholera toxin 16 hours before performing the experiment. Where indicated, cells were pre-treated for 2 h with 75 μM EIPA before incubation with 1 mg/ml TMR-dextran, 70,000 MW and the stimulation mix (100 ng/ml EGF, 100 ng/ml HGF, 100 ng/ml AREG and 100 ng/ml HRG1-β1) for 1 h at 37°C. Next, cells were washed four times with ice-cold PBS, fixed in 4% paraformaldehyde (in PBS) for 10 min, washed four times with PBS, and processed for widefield analysis. Each assay was done in triplicate and at least 150 cells were counted in each experiment.

Single cell random motility assay

Single cells migration was monitored in normal growing conditions. Briefly, cells were seeded sparsely in a 6-well plate ($2*10^4$ cells/well) in complete media supplemented with 20 ng/ml EGF. Doxycycline (2.5 μg/ml) was added to the media 16 hours before starting the experiment. Random cell motility was monitored over a 24 hours period. Pictures were taken every 5 minutes from 10 positions/condition, using a motorized Olympus Scan^R inverted microscope with 10X objective. All the experiments were performed using an environmental microscope incubator set to 37°C and 5% CO2 perfusion. Single cells were manually tracked using Manual Tracking Tool ImageJ software plugin. Migration plot and relative parameters were obtained by Chemotaxis and Migration Tool ImageJ software plugin.

AFM indentation method

Doxycycline-induced control and RAB5A-MCF-10A monolayers were seeded on 24 mm diameter coverslip at a jamming density before AFM indentation experiment. AFM indentation was carried out using JPK NanoWizard3 mounted on an Olympus inverted microscope. The protocol was adapted from previous study [7]. A modified AFM tip (NovaScan, USA) attached with 10 μm diameter bead was used to indent the center of the cell. The spring constant of the AFM tip cantilever is 0.03 N/m. AFM indentation loading rate is 0.5 Hz with a ramp size of 3 μm. AFM Indention force was set at a threshold of 2nN. The data points below 0.5 μm indentation depth were used to calculate Young's modulus to ensure small deformation and minimize substrate contributions [7]. The Hertz model is shown below:

$$F = \frac{4}{3}\frac{E}{(1-\nu^2)}\sqrt{R\delta^3}$$

where F is the indentation force, E is the Young's modulus to be determined, ν is the Poisson's ratio, R is the radius of the spherical bead, and δ is indentation depth. The cell was assumed incompressible and a Poisson's ratio of 0.5 was used.

Laser nanoscissors

Nanoscissor experiments were performed on a Leica SP5 confocal microscope. Images were acquired with a Plan-Apochromat 63×/1.4 NA oil-immersion objective at 2× digital zoom (λ_{exc} = 488nm; scan frequency 700Hz). A total of 5 frames were acquired with an interval of 15 s per frame. The Ti-sapphire laser (Chameleon 2; Coherent Scientific, US) was tuned to 790 nm (20% laser transmission) for the ablation of cell–cell contacts labeled with Ecad-GFP and the Leica point-bleach tool was used to focalize the beam on a single pixel on the cell–cell contact (pixel dwell time 50 ms).

The distance (d) between vertices that define the ablated con- tact was measured as a fraction of time (t). Distance values after ablation were subtracted from the initial contact length, *d(0)*. The values of $[d(t) – d(0)]/2$ were then calculated as a function of time, and initial recoil values for each contact were obtained by nonlinear regression of the data to the following equation:

$f(t)= (\text{initial recoil}/k)(1–e^{-kt})$

Finally, statistical analysis for control-normalized average initial recoil between different groups was performed by *t* test as described in the corresponding figure caption.

FRAP analysis

Cells were seeded on glass coverslips and cultured in complete medium until a uniform monolayer had formed. RAB5A expression was doxycycline-induced 16 hours before performing the experiment and cell culture medium has been refreshed before the live-imaging session.

FRAP experiments were performed on an UltraVIEW VoX spinning-disk confocal system (PerkinElmer) equipped with an EclipseTi inverted microscope (Nikon) provided with a Nikon Perfect Focus System, an integrated FRAP PhotoKinesis unit (PerkinElmer) and a Hamamatsu CCD camera (C9100-50) and driven by Volocity software (Improvision; Perkin Elmer). All images were acquired through a 60X oil-immersion objective (Nikon Plan Apo VC, NA 1.4). The photobleaching was performed using a rectangular region (3x8 µm) on the cell junctions. After defining the region of interest, the 488 nm was used at the maximum power for 30 bleaching cycles to bleach GFP signal. After bleaching, images were acquired every 4 seconds for the first 10 minutes and every 10 seconds for the last 5 minutes. A custom ImageJ macro and a set of functions written in Matlab (MathWorks) software were used to analyse the recovery curves. Briefly, the mean intensity value in the bleached area was measured, corrected for the background and for the acquisition photobleaching and the curves were then normalized to the pre-bleaching mean intensity values. A single exponential function was used to fit the recovery curves.

Zebrafish strains and maintenance

Zebrafish (*Danio rerio*) embryos obtained from natural spawning of wild type strain *AB*, were raised according to standard procedures and bred according to the national guidelines (Italian decree "4 march 2014, n.26"). Developmental stages of the embryos were classified according to morphological criteria [8]. All experimental procedures were approved by the FIRC Institute of Molecular Oncology Institutional Animal Care and Use Committee and approved by the Ministry of Health (Authorization number: 219/2106-PR).

RAB5A mRNA preparation and injection in zebrafish embryos

mRNA of human RAB5A fused with CFP reporter at N-terminus (CFP:hRAB5A) was synthesized from *pCS2+-PRDM5* vector previously linearized with *NotI* restriction enzyme[9]. 1 μg of linearized vector was *in vitro* transcribed with SP6 using the *mMessage Machine* kit (Ambion). Embryos were microinjected at 1-cell stage using 200 pg of synthetic CFP:hRAB5A capped mRNA and let to grow in E3 medium at 28.5°C together with not injected embryos.

***In vivo* analysis of epiboly progression**

After 5.5 hours post fertilization (hpf), using a fluorescence stereomicroscope we selected about 30 injected embryos on the basis of CFP expression and about 30 not injected embryos then, thanks to stereomicroscope analysis, we classified and annotated their developmental stages (about 50% of epiboly) blindly. After 3 hours (8.5 hpf), we evaluated the progression of the epiboly of the same embryos at the standard temperature of 28.5°C. We performed two independent experiments and all data were statistically analyzed using Student's t-test and plotted.

Zebrafish time-lapse movie analysis

Two live embryos at 50% of epiboly stage (one expressing CFP:hRAB5A and one not injected) were manually de-chorionated and mounted, in lateral position, in 1% low-melting agarose in E3 water. Images were acquired every 5 minutes by Nikon Eclipse 90i microscope and 4x objective and time-lapse movie with duration of 3 hours was created by "NIS-Elements" software (Nikon). We performed two independent analysis.

Statistical analysis

Student's unpaired t or non-parametric Mann–Whitney-U tests were used for determining the statistical significance. Significance was defined as $*p < 0.05$; $**p < 0.01$; $***p < 0.001$ and $****p$

< 0.0001. Statistic calculations were performed with GraphPad Prism Software. Data are expressed as mean ± SEM, unless otherwise indicated.

5. Supplementary References

1. Bergert, M. *et al.* Confocal reference free traction force microscopy. *Nature communications* **7**, 12814 (2016).
2. Tambe, D.T. *et al.* Collective cell guidance by cooperative intercellular forces. *Nature materials* **10**, 469-475 (2011).
3. Bi, D., Yang, X., Marchetti, M.C. & Manning, M.L. Motility-Driven Glass and Jamming Transitions in Biological Tissues. *Physical Review X* **6**, 021011 (2016).
4. Park, J.A. *et al.* Unjamming and cell shape in the asthmatic airway epithelium. *Nature materials* **14**, 1040-1048 (2015).
5. Szabo, B. *et al.* Phase transition in the collective migration of tissue cells: experiment and model. *Phys Rev E Stat Nonlin Soft Matter Phys* **74**, 061908 (2006).
6. Beznoussenko, G.V. & Mironov, A.A. Correlative video-light-electron microscopy of mobile organelles. *Methods Mol Biol* **1270**, 321-346 (2015).
7. Li, Q.S., Lee, G.Y., Ong, C.N. & Lim, C.T. AFM indentation study of breast cancer cells. *Biochem Biophys Res Commun* **374**, 609-613 (2008).
8. Kimmel, C.B., Ballard, W.W., Kimmel, S.R., Ullmann, B. & Schilling, T.F. Stages of embryonic development of the zebrafish. *Dev Dyn* **203**, 253-310 (1995).
9. Palamidessi, A. *et al.* Endocytic trafficking of Rac is required for the spatial restriction of signaling in cell migration. *Cell* **134**, 135-147 (2008).